



Contents lists available at ScienceDirect

Journal of Cardiovascular Computed Tomography

journal homepage: www.JournalofCardiovascularCT.com

Research paper

Prognostic value of a novel artificial intelligence-based coronary CTA-derived ischemia algorithm among patients with normal or abnormal myocardial perfusion

Sarah Bär^{a,b}, Teemu Maaniitty^{a,d}, Takeru Nabeta^c, Jeroen J. Bax^c, James P. Earls^f, James K. Min^f, Antti Saraste^{a,e}, Juhani Knuuti^{a,d,*}

^a Turku PET Centre, Turku University Hospital and University of Turku, Turku, Finland

^b Department of Cardiology, Bern University Hospital Inselspital, Bern, Switzerland

^c Department of Cardiology, Leiden University Medical Center, Leiden, The Netherlands

^d Department of Clinical Physiology, Nuclear Medicine, and PET, Turku University Hospital, Turku, Finland

^e Heart Center, Turku University Hospital and University of Turku, Turku, Finland

^f Cleerly inc., New York, United States

ARTICLE INFO

Keywords:

Coronary computed tomography angiography

Artificial intelligence

Positron emission tomography

Ischemia

Prognosis

ABSTRACT

Background: Among patients with obstructive coronary artery disease (CAD) on coronary computed tomography angiography (CTA), downstream positron emission tomography (PET) perfusion imaging can be performed to assess the presence of myocardial ischemia. A novel artificial-intelligence-guided quantitative computed tomography ischemia algorithm (AI-QCT_{ischemia}) aims to predict ischemia directly from coronary CTA images. We aimed to study the prognostic value of AI-QCT_{ischemia} among patients with obstructive CAD on coronary CTA and normal or abnormal downstream PET perfusion.

Methods: AI-QCT_{ischemia} was calculated by blinded analysts among patients from the retrospective coronary CTA cohort at Turku University Hospital, Finland, with obstructive CAD on initial visual reading (diameter stenosis $\geq 50\%$) being referred for downstream ¹⁵O-H₂O-PET adenosine stress perfusion imaging. All coronary arteries with their side branches were assessed by AI-QCT_{ischemia}. Absolute stress myocardial blood flow ≤ 2.3 ml/g/min in ≥ 2 adjacent segments was considered abnormal. The primary endpoint was death, myocardial infarction, or unstable angina pectoris. The median follow-up was 6.2 [IQR 4.4–8.3] years.

Results: 662 of 768 (86%) patients had conclusive AI-QCT_{ischemia} result. In patients with normal ¹⁵O-H₂O-PET perfusion, an abnormal AI-QCT_{ischemia} result (n = 147/331) vs. normal AI-QCT_{ischemia} result (n = 184/331) was associated with a significantly higher crude and adjusted rates of the primary endpoint (adjusted HR 2.47, 95% CI 1.17–5.21, p = 0.018). This did not pertain to patients with abnormal ¹⁵O-H₂O-PET perfusion (abnormal AI-QCT_{ischemia} result (n = 269/331) vs. normal AI-QCT_{ischemia} result (n = 62/331); adjusted HR 1.09, 95% CI 0.58–2.02, p = 0.794) (p-interaction = 0.039).

Conclusion: Among patients with obstructive CAD on coronary CTA referred for downstream ¹⁵O-H₂O-PET perfusion imaging, AI-QCT_{ischemia} showed incremental prognostic value among patients with preserved perfusion by ¹⁵O-H₂O-PET imaging, but not among those with reduced perfusion.

1. Introduction

Coronary computed tomography angiography (CTA) represents the first-line non-invasive imaging technique for the detection of coronary

artery disease (CAD) among patients with low to intermediate pre-test probability of CAD.^{1,2} However, as per current guidelines,^{1,2} coronary revascularization mandates the presence of myocardial ischemia. Therefore, hybrid or sequential functional approaches such as

Abbreviations: AI, artificial intelligence; AI-QCT, artificial intelligence-guided quantitative computed tomography; AI-QCT_{ischemia}, artificial intelligence-guided quantitative computed tomography ischemia algorithm; CPV, calcified plaque volume; ICA, invasive coronary angiography; MBF, myocardial blood flow; NCPV, non-calcified plaque volume; PAV, percent atheroma volume.

* Corresponding author. Turku PET Centre, Turku University Hospital, P.O.Box 52 FI-20521, Turku, Finland.

E-mail address: juhani.knuuti@utu.fi (J. Knuuti).

<https://doi.org/10.1016/j.jcct.2024.04.001>

Received 13 December 2023; Received in revised form 11 April 2024; Accepted 11 April 2024

1934-5925/© 2024 Published by Elsevier Inc. on behalf of Society of Cardiovascular Computed Tomography. This is an open access article under the CC BY license (<http://creativecommons.org/licenses/by/4.0/>).

myocardial perfusion imaging to combine anatomical and functional information on the extent of CAD, are currently being used in clinical practice.

Several studies have shown that the objective and reproducible artificial intelligence (AI) based quantitative computed tomography (AI-QCT) analysis achieves high diagnostic accuracy for both obstructive stenosis detection and atherosclerotic plaque burden quantification.³⁻⁶ Also, AI-QCT plaque analysis has been shown to provide prognostic information.⁷ Recently, a novel AI-based quantitative computed tomography algorithm (AI-QCT_{ischemia}), which aims to predict the probability of myocardial ischemia directly from coronary CTA images, has been developed and received clearance by the U.S. Food and Drug Administration (FDA) (Clearly ISCHEMIA, Clearly Inc, Denver CO, USA⁸). AI-QCT_{ischemia} uses 37 morphological coronary CTA variables from AI-QCT and was trained against invasive fractional flow reserve (FFR) with cut-off 0.80 using data from the CREDESCENCE (Computed Tomographic evaluation of atherosclerotic DEterminants of myocardial IsChemia)⁹ trial (50:50 derivation and internal validation) and has undergone external validation using data from the PACIFIC (Prospective Comparison of Cardiac PET/CT, SPECT/CT Perfusion Imaging and CT Coronary Angiography With Invasive Coronary Angiography)¹⁰ trial. Its agreement with FFR ≤ 0.80 was similar to that of ¹⁵O-H₂O positron emission tomography (¹⁵O-H₂O-PET) and significantly higher as for CT-based FFR (FFR-CT) and single photon emission computed tomography.¹¹ However, the prognostic value of AI-QCT_{ischemia} among patients with an indication for functional evaluation after coronary CTA is currently unknown. Therefore, we aimed to investigate the added risk stratification of AI-QCT_{ischemia} among patients with visual obstructive stenosis and normal or abnormal perfusion according to the non-invasive gold standard ¹⁵O-H₂O-PET.

2. Methods

2.1. Patient population and follow-up

A total of 2411 patients with suspected CAD were referred for coronary CTA from February 2007 to December 2016. According to the institutional protocol, for patients with no or non-obstructive CAD on coronary CTA, further imaging is not required, whereas patients with visual obstructive CAD (adapting the criterion of $\geq 50\%$ stenosis) are referred for downstream adenosine stress myocardial PET perfusion imaging.^{12,13} The outcome according to AI-QCT_{ischemia} of the total cohort as well as for patients with anatomically no or non-obstructive disease (visual stenosis $\leq 50\%$) has been reported previously.¹⁴ For this analysis, 1037 patients from this cohort with visually obstructive CAD undergoing downstream PET perfusion imaging after coronary CTA were eligible. No patient did previously undergo coronary revascularization, had known obstructive CAD (i.e. $>50\%$ diameter stenosis by invasive coronary angiography (ICA)), or did undergo PET-CT for another indication (e.g. cardiomyopathy or heart failure). Additionally, 137 patients were excluded due to unavailable CTA image data, 97 due to non-adherence to the imaging protocol, 32 due to a non-diagnostic imaging study, and 3 were lost to follow-up. Thus, the final study population consisted of 768 patients eligible for AI-QCT_{ischemia} analysis (Fig. 1). Data on clinical characteristics, symptoms, and medication were retrospectively collected from electronic medical records. Comprehensive data on all-cause death, myocardial infarction (MI), and unstable angina pectoris (uAP) were recorded using the registries of the Finnish National Institute for Health and Welfare and the Centre for Clinical Informatics of the Turku University Hospital. The events identified from the registries were confirmed by investigators using electronic medical records. The follow-up time was

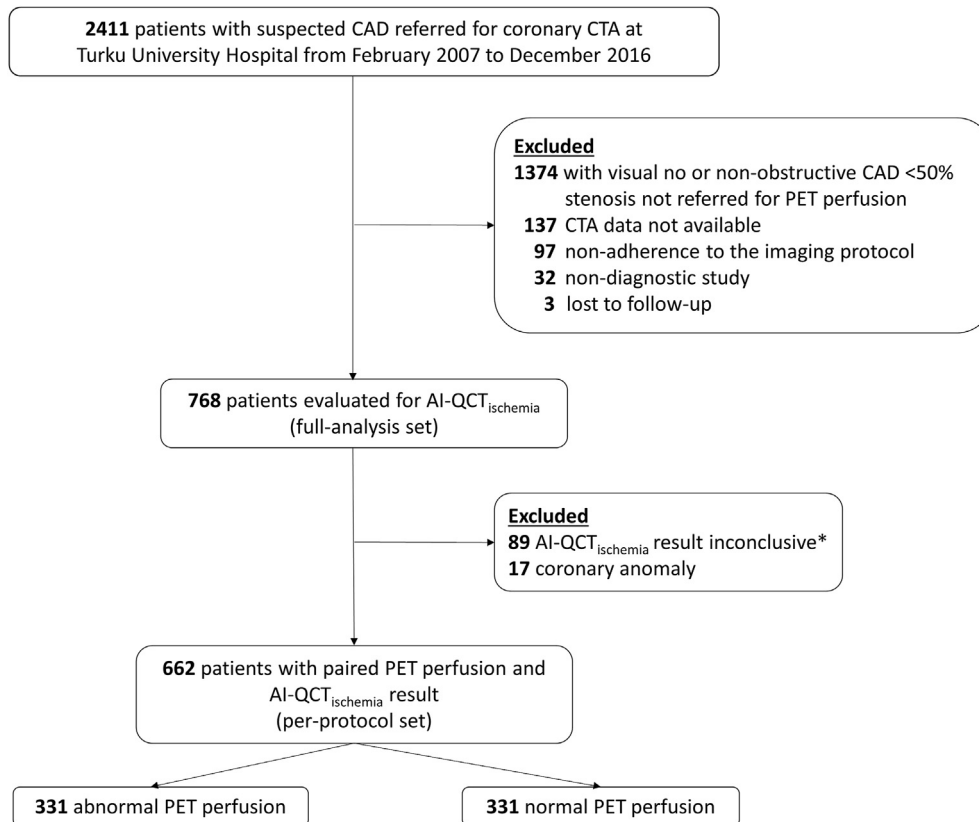


Fig. 1. Patient Flowchart. *AI-QCT_{ischemia} was classified inconclusive if the result was not available for all vessels in the absence of any ischemic vessels. AI-QCT = artificial intelligence quantitative computed tomography, CAD = coronary artery disease, CTA = computed tomography angiography, PET = positron emission tomography.

median 6.2 [interquartile range (IQR) 4.4–8.3] years. The study conforms with the Declaration of Helsinki. The Ethics Committee of the Hospital District of Southwest Finland approved the study protocol and waived the need for written informed consent.

2.2. Coronary CTA and $^{15}\text{O-H}_2\text{O}$ PET imaging procedures

Coronary CTA and PET imaging was performed according to the recommendations valid during the enrollment period.¹⁵ In brief, coronary CTA scans were performed with 64-row hybrid PET-CT scanner (GE Discovery VCT or GE D690, General Electric Medical Systems, Waukesha, United States). Before coronary CTA image acquisition, intravenous metoprolol (0–30 mg) to achieve a target heart rate of 60 beats/min, as well as isosorbide dinitrate aerosol (1.25 mg) or sublingual nitrate (800 mg) were administered. Coronary CTA was performed using intravenously administered low-osmolal iodine contrast agent. Prospectively triggered acquisition was applied whenever feasible. A dynamic quantitative PET perfusion scan during adenosine stress was carried out using a hybrid PET-CT device in the same imaging session, as previously described.¹⁵ ^{15}O -labeled water ($^{15}\text{O-H}_2\text{O}$) was used as a radiotracer and adenosine infusion (140 $\mu\text{g}/\text{kg}/\text{min}$) was used for vasodilator stress (stress-only protocol).¹⁵

The patients were instructed to abstain from caffeine for 24 h before PET imaging. In some patients, perfusion imaging was performed in the following days or weeks due to logistical reasons or caffeine use.

Coronary CTA data were initially analyzed visually according to the American Heart Association (AHA) recommendations valid during the enrollment period¹⁶ by experienced clinical readers including vessels with diameter ≥ 1.5 mm. This initial visual CTA analysis acted as a gatekeeper for downstream PET referral. PET data were quantitatively analyzed using Carimas software version 1.0–2.10 (developed at Turku PET Centre, Turku, Finland) to measure stress myocardial blood flow (MBF) in standardized 17 segments according to AHA recommendations.^{15,17} Absolute stress MBF ≤ 2.3 ml/g/min in at least 2 adjacent myocardial segments was considered abnormal based on previous validation against invasive FFR.¹⁸

2.3. AI-QCT_{ischemia} algorithm

Coronary CTA scans from our retrospective patient cohort were re-analyzed in 2022–2023 in a blinded manner using a previously

described AI-QCT algorithm (Clearly LABS, Clearly Inc, Denver CO).^{3,4} This commercially available FDA-cleared software utilizes a series of validated convolutional neural networks (3D U-Net and VGG network variants) for image quality assessment, coronary segmentation and labeling, lumen wall evaluation and vessel contour determination, and plaque characterization. The quantitative output of the AI-QCT algorithm consists of presence or absence of features of: 1) stenosis parameters, such as diameter stenosis (%) and area stenosis (%), number of severe stenosis $>70\%$ and number of moderate stenosis 50–70%, 2) atherosclerosis measurements, such as non-calcified plaque volume, total plaque volume, lesion length, 3) vascular morphology features such as total vessel volume, total lumen volume and vessel length and 4) diffuseness that includes a calculation of the sum of volumes and lengths across all involved segments. The AI-QCT results are then fed into the FDA-cleared AI-QCT_{ischemia} algorithm (Clearly ISCHEMIA, Clearly Inc, Denver CO⁸). AI-QCT_{ischemia} is a method to determine the probability of an abnormal invasive FFR ≤ 0.80 from coronary CTA data using a random forest machine learned algorithm incorporating 37 coronary CTA-derived quantitative variables from AI-QCT.¹¹ All coronary arteries with their side branches with diameter ≥ 1.5 mm are evaluated by the algorithm according to the Society of Cardiovascular Computed Tomography (SCCT) 18-segment system.¹⁹ AI-QCT_{ischemia} automatically selects the image series per vessel with the best quality. AI-QCT_{ischemia} cannot be calculated in case of coronary anomalies (except for absent left main), the presence of stents (not relevant to the current population with native coronary arteries), or if $>15\%$ downstream of a vessel cannot be evaluated. The final output is a calculation by a machine learned algorithm to provide non-invasive estimates of FFR, as categorized by professional societal guideline-indicated thresholds of ischemia likely (≤ 0.80 invasive FFR) vs. ischemia unlikely (>0.80 invasive FFR).^{1,2} These results are then presented to the end user in binary fashion (i.e. abnormal AI-QCT_{ischemia} result or normal AI-QCT_{ischemia} result) for ease of understanding for non-specialists and to be in direct accordance with the guideline recommended thresholds to guide coronary revascularization or deferral (Fig. 2). Given that coronary ischemia in a proximal portion of a vessel naturally propagates distally, segments distal to a point along the same vessel tree, where the AI-QCT_{ischemia} result becomes abnormal, are also classified as having an abnormal AI-QCT_{ischemia} result.¹¹ As such, e.g. left main disease is reflected in both its downstream vessels (e.g. left anterior descending artery and left circumflex artery).¹¹

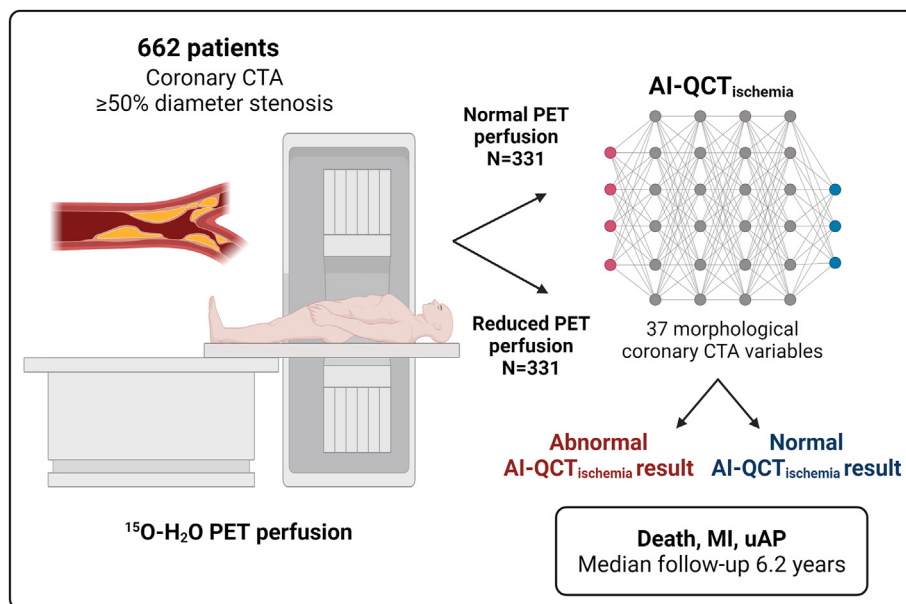


Fig. 2. Study Design. AI-QCT = artificial intelligence quantitative computed tomography, CAD = coronary artery disease, CTA = computed tomography angiography, MI = myocardial infarction, PET = positron emission tomography, uAP = unstable angina pectoris. Created with BioRender.com.

For the current study, patients were classified as having an abnormal AI-QCT_{ischemia} result in case ≥ 1 vessel or side branch was ischemic based on the algorithm. Patients were classified as having a normal AI-QCT_{ischemia} result in case all main coronary arteries (left main, left anterior descending artery, left circumflex artery, right coronary artery) and side branches were analyzable and non-ischemic according to the algorithm. If there was ≥ 1 non-evaluable vessel in the absence of any ischemic vessels, patients were considered as inconclusive by AI-QCT_{ischemia} and excluded from the per-protocol analysis. In the full-analysis set, these patients were assessed in an intention-to-diagnose approach, i.e. by classifying those with an inconclusive AI-QCT_{ischemia} result as having an abnormal AI-QCT_{ischemia} result.

2.4. Primary endpoint

The primary endpoint was the composite of death, MI, or uAP among patients with an abnormal vs. a normal AI-QCT_{ischemia} result. This endpoint was assessed separately among patients with normal or abnormal stress MBF in ¹⁵O-H₂O-PET. MIs were type 1 MIs,²⁰ and uAP was defined according to the standard definition.²¹

2.5. Statistical analysis

The statistical analyses were performed in an independent academic setting at Turku University Hospital. Continuous variables are shown as mean \pm standard deviation (SD) or median (IQR [25th to 75th percentile]). Categorical variables are shown as numbers with percentages. Student's T test or Mann Whitney U test were used to compare continuous variables and 2-sided Chi-square test was used for categorical variables. Kaplan-Meier curves for clinical events were created and compared with the log-rank test between patients with a normal vs. abnormal AI-QCT_{ischemia} result separately among patients with normal or abnormal stress MBF. We report crude hazard ratios (HR) from univariable and adjusted HRs (HR_{adj}) from multivariable Cox proportional hazards models. Analyses were censored at 10 years due to the low number of patients at risk after 10 years. Adjusting covariates were chosen based on clinical reasoning and consisted of age, sex, hypertension, diabetes mellitus, smoking, dyslipidemia, family history of CAD, and typical angina. Variables with a significant association in univariable models were included into the multivariable models. Analyses were two-tailed and a p-value < 0.05 was considered statistically significant. All analyses were performed in Stata version 15 (StataCorp. 2017. Stata Statistical Software: Release 15. College Station, TX: StataCorp LLC).

3. Results

3.1. Patient population

Out of 768 patients with available coronary CTA and PET perfusion data (full analysis set), 17 patients were excluded due to coronary anomalies and 89 patients due to inconclusive AI-QCT_{ischemia}, resulting in 662 (86%) patients with evaluable AI-QCT_{ischemia} result (per-protocol set) (Fig. 1). Of these, 331 (50.0%) patients had abnormal and 331 (50.0%) patients had normal PET perfusion. Characteristics of patients with abnormal vs. normal PET perfusion are shown in Table S1.

In the group with normal PET perfusion (n = 331) (Table 1), 147 (44.4%) had an abnormal and 184 (55.6%) had a normal AI-QCT_{ischemia} result. The prevalence of cardiovascular risk factors and medical therapy was similar between those with an abnormal as compared to those with a normal AI-QCT_{ischemia} result. However, patients with an abnormal AI-QCT_{ischemia} result were slightly younger (66 vs. 68 years, p < 0.001), were more frequently referred for ICA (26.5% vs. 7.6%, p < 0.001) and underwent more frequently early elective revascularization within 6 months (11.6% vs. 0.5%, p < 0.001).

Also, they had higher Agatston calcium score (407 vs. 124, p < 0.001) and AI-QCT diameter stenosis (59% vs. 31%, p < 0.001), more frequently

$\geq 50\%$ diameter stenosis by AI-QCT (93.9% vs. 8.7%, p < 0.001), higher percent atheroma volume (PAV) (13.8% vs. 6.1%, p < 0.001), percent calcified plaque volume (CPV) (5.6% vs. 1.6%, p < 0.001, and percent non-calcified plaque volume (NCPV) (7.4% vs. 3.8%, p < 0.001).

In the group with abnormal PET perfusion (n = 331) (Table 2), 269 (81.3%) had an abnormal and 62 (18.7%) had a normal AI-QCT_{ischemia} result. Clinical characteristics between those with an abnormal vs. normal AI-QCT_{ischemia} result were similar. However, patients with an abnormal AI-QCT_{ischemia} result were more frequently prescribed an antiplatelet agent (61.7% vs. 41.9%, p < 0.001), were more frequently referred for ICA (68.4% vs. 35.5%, p < 0.001) and underwent more frequently early revascularization (50.9% vs. 17.7%, p < 0.001). Also, they had higher Agatston calcium score (656 vs. 194, p < 0.001) and AI-QCT diameter stenosis (72% vs. 36%, p < 0.001) more frequently $\geq 50\%$ diameter stenosis by AI-QCT (95.2% vs. 14.5%, p < 0.001), higher PAV (18.9% vs. 7.9%, p < 0.001), CPV (6.8% vs. 2.0%, p < 0.001), and NCPV (10.1% vs. 5.6%, p < 0.001).

3.2. Primary endpoint in normal PET perfusion group

In the group with normal PET perfusion (n = 331), 17.0% (n = 25/147) of patients with an abnormal AI-QCT_{ischemia} result and 5.4% (n = 10/184) of patients with a normal AI-QCT_{ischemia} result experienced the primary endpoint. The crude rate of the primary endpoint was significantly higher among patients with an abnormal vs. normal AI-QCT_{ischemia} result (HR 3.11, 95% CI 1.49–6.47, p = 0.002) (Fig. 3, Table 3). Results remained consistent after adjusting for age and diabetes mellitus according to significant associations with the primary endpoint in univariable models (Table S2) (HR_{adj} 2.47, 95% CI 1.17–5.21, p = 0.018) (Table 3). The rate of death alone was non-significantly different between the groups (HR 2.37, 95% CI 0.95–5.88, p = 0.064) (Table 3, Table S3). The crude rate of MI alone was higher for patients with an abnormal AI-QCT_{ischemia} result (HR 5.08, 95% CI 1.43–18.00, p = 0.012) and remained significant after adjusting for age (HR_{adj} 3.93, 95% CI 1.10–14.07, p = 0.036) (Table 3, Table S4). uAP alone could not be compared between groups, since none occurred in the group with a normal AI-QCT_{ischemia} result (Table 3).

Analyses censored at 2 and 6 years showed that the rate of the primary endpoint starts to diverge between the AI-QCT_{ischemia} groups from 6 years of follow-up onwards (Table S5).

The main analysis was repeated in the full-analysis set as an intention-to-diagnose approach, i.e. classifying those patients with an inconclusive AI-QCT_{ischemia} (n = 64) as having an abnormal AI-QCT_{ischemia} result. This analysis remained consistent with the main results (Table S6).

3.3. Primary endpoint in abnormal PET perfusion group

In the group with abnormal PET perfusion (n = 331), 21.9% (n = 59/269) of patients with an abnormal AI-QCT_{ischemia} result and 19.4% (n = 12/62) of patients with a normal AI-QCT_{ischemia} result experienced the primary endpoint. There was no significant difference in the crude rate of the primary endpoint (HR 1.14, 95% CI 0.61–2.12, p = 0.679) (Fig. 3, Table 3). Results remained consistent after adjusting for age according to a significant association with the primary endpoint in the univariable model (Table S2) (HR_{adj} 1.09, 95% CI 0.58–2.02, p = 0.794) (Table 3). There were also no significant differences in the rates of death or MI alone between groups (death: HR 0.57, 95% CI 0.28–1.13, p = 0.108; MI: 4.83, 95% CI 0.65–35.93, p = 0.124). uAP alone could not be compared between groups, since none occurred in the group with a normal AI-QCT_{ischemia} result (Table 3). Analyses censored at 2 and 6 years showed similar results (Table S5).

Results of the full-analysis set (i.e. classifying 42 patients with inconclusive AI-QCT_{ischemia} as having an abnormal AI-QCT_{ischemia} result) remained consistent with the main results (Table S6).

Table 1
Baseline characteristics of patients with normal PET perfusion.

Clinical characteristics	N	Abnormal AI-QCT _{ischemia} result (N = 147)	N	Normal AI-QCT _{ischemia} result (N = 184)	p-value
Age, years	147	66 [59–71]	184	68 [64–73]	<0.001
Sex (male), n (%)	147	71 (48.3%)	184	86 (46.7%)	0.778
Hypertension, n (%)	147	109 (74.2%)	184	119 (64.7%)	0.064
Dyslipidemia, n (%)	147	105 (71.4%)	184	127 (69.0%)	0.635
Current smoker, n (%)	147	17 (11.6%)	184	22 (12.0%)	0.913
Previous smoker, n (%)	147	41 (27.9%)	184	45 (24.5%)	0.479
BMI, kg/m ²	139	27.5 [24.8–30.1]	166	27.3 [24.8–30.9]	0.898
Diabetes mellitus, n (%)	147	33 (22.5%)	184	33 (17.9%)	0.307
Prediabetes ^a , n (%)	147	16 (10.9%)	184	35 (19.0%)	0.042
Family history of CAD, n (%)	147	70 (47.6%)	184	81 (44.0%)	0.514
Typical angina pectoris, n (%)	147	33 (22.5%)	184	42 (22.8%)	0.935
NYHA class	101		117		0.049
I		51 (50.5%)		73 (62.4%)	
II		39 (38.6%)		40 (34.2%)	
III		11 (10.9%)		4 (3.4%)	
Agatston Coronary Calcium Score	118	407 [224–980]	160	124 [33–259]	<0.001
Referral for ICA (within 6 months), n (%)	147	39 (26.5%)	184	14 (7.6%)	<0.001
Early revascularization (within 6 months, PCI or CABG), n (%)	147	17 (11.6%)	184	1 (0.5%)	<0.001
Early PCI (within 6 months), n (%)	147	17 (11.6%)	184	1 (0.5%)	<0.001
Early CABG (within 6 months), n (%)	147	–	184	–	–
Medication					
Antiplatelet drug (Aspirin or other), n (%)	147	74 (50.3%)	184	77 (41.9%)	0.123
Anticoagulation, n (%)	147	19 (12.9%)	184	14 (7.6%)	0.109
Lipid-lowering drug, n (%)	147	72 (49.0%)	184	85 (46.2%)	0.614
Beta blocker, n (%)	147	76 (51.7%)	184	90 (48.9%)	0.614
Long-acting nitrate, n (%)	147	15 (10.2%)	184	21 (11.4%)	0.726
Calcium channel blocker, n (%)	147	32 (21.8%)	184	36 (19.6%)	0.622
ACE inhibitor, n (%)	147	31 (21.1%)	184	35 (19.0%)	0.640
AT II antagonist, n (%)	147	33 (22.5%)	184	46 (25.0%)	0.589
Diuretic, n (%)	147	38 (25.9%)	184	35 (19.0%)	0.137
Antiarrhythmic drug, n (%)	147	5 (3.4%)	184	5 (2.7%)	0.718
AI-QCT					
AI-QCT diameter stenosis, %	147	59 [54–71]	184	31 [23–41]	<0.001
AI-QCT diameter stenosis $\geq 30\%$, n (%)	147	147 (100%)	184	103 (56.0%)	<0.001
AI-QCT diameter stenosis $\geq 50\%$, n (%)	147	138 (93.9%)	184	16 (8.7%)	<0.001
AI-QCT diameter stenosis $\geq 70\%$, n (%)	147	40 (27.2%)	184	0 (0.0%)	<0.001
Vessels with AI-QCT diameter stenosis $\geq 50\%$ ^b , n (%)					
LM	144	5 (3.5%)	181	0 (0.0%)	0.012
LAD	147	113 (76.9%)	184	12 (6.7%)	<0.001
LCX	147	20 (13.6%)	184	3 (1.6%)	<0.001
RCA	147	40 (27.2%)	184	3 (1.6%)	<0.001
Area stenosis, %	147	84 [79–92]	184	58 [47–69]	<0.001
Percent atheroma volume, %	147	13.8 [8.8–20.3]	184	6.1 [3.3–9.3]	<0.001
Percent calcified plaque volume, %	147	5.6 [2.6–9.9]	184	1.6 [0.4–3.6]	<0.001
Percent non-calcified plaque volume, %	147	7.4 [5.3–10.5]	184	3.8 [2.5–5.9]	<0.001
Positive remodeling ^c , n (%)	147	147 (100%)	184	182 (98.9%)	0.205
Total vessel volume, mm ³	147	3162 [2652–3814]	184	3168 [2640–3811]	0.700
Total lumen volume, mm ³	147	2621 [2187–3250]	184	2909 [2404–3534]	0.006
Total vessel length, mm	147	616 \pm 105	184	632 \pm 89	0.135

Values are n (%), mean \pm standard deviation (SD) or median [interquartile range (IQR)]. P-values are Mann Withney U tests, T-tests, or Chi-square tests.

^a Prediabetes was defined as HbA1c 6.0–6.5%, or fasting glucose 6.1–6.9 mmol/l or impaired glucose tolerance (2 h plasma glucose 7.8–11.0 mmol/l in a 75 oral glucose tolerance test).

^b Including side branches with diameter ≥ 1.5 mm. In some patients, left main was either absent or too short to be assessed as separate segment.

^c Remodeling index ≥ 1.1 . Percent plaque volume (%) = plaque volume (mm³)/vessel volume (mm³)*100. AI-QCT = artificial intelligence quantitative computed tomography, ACE = angiotensin converting enzyme, AP = angina pectoris, AT II = angiotensin II, BMI = body mass index, CABG = coronary artery bypass grafting, CAD = coronary artery disease, ICA = invasive coronary angiography, LAD = left anterior descending, LCX = left circumflex artery, LM = left main artery, NYHA = New York Heart Association, PCI = percutaneous coronary intervention, PET = positron emission tomography, RCA = right coronary artery.

3.4. Sensitivity analysis without patients undergoing early revascularization

Overall, 25.1% (n = 166/662) of patients underwent early revascularization within 6 months. 31 patients (18.7%) who underwent early revascularization and 75 (15.1%) of patients who did not undergo early revascularization experienced the primary endpoint and event rates were similar (HR 1.15, 95% CI 0.75–1.74, p = 0.523). The main analysis was repeated among the 496 patients without early revascularization and results were consistent. Among patients with normal PET perfusion (n = 313), 16.9% (n = 22/130) of patients with an abnormal AI-QCT_{ischemia} result and 5.5% (n = 10/183) of patients with a normal

AI-QCT_{ischemia} result experienced the primary endpoint. The crude and adjusted rates of the primary endpoint were significantly higher for patients with an abnormal as compared to a normal AI-QCT_{ischemia} result (HR_{adj} 2.70, 95% CI 1.26–5.80, p = 0.011) (Table S7). Among patients with abnormal PET perfusion (n = 183), 25.0% (n = 33/132) of patients with an abnormal AI-QCT_{ischemia} result and 19.6% (n = 10/51) of patients with a normal AI-QCT_{ischemia} result experienced the primary endpoint. The crude rate of the primary endpoint was similar for patients with an abnormal vs. normal AI-QCT_{ischemia} result (HR 1.35, 95% CI 0.66–2.74, p = 0.407). Adjusted analyses were not performed, since none of the variables showed a significant association with the primary endpoint (Table S7).

Table 2
Baseline characteristics of patients with abnormal PET perfusion.

Clinical characteristics	N	Abnormal AI-QCT _{ischemia} result (N = 269)	N	Normal AI-QCT _{ischemia} result (N = 62)	p-value
Age, years	269	66 [60–71]	62	65 [57–69]	0.162
Sex (male), n (%)	269	188 (69.9%)	62	40 (64.5%)	0.410
Hypertension, n (%)	269	182 (67.6%)	62	42 (67.7%)	0.990
Dyslipidemia, n (%)	269	203 (75.5%)	62	46 (74.2%)	0.834
Current smoker, n (%)	269	38 (14.1%)	62	12 (19.4%)	0.300
Previous smoker, n (%)	269	77 (28.6%)	62	20 (32.3%)	0.571
BMI, kg/m ²	251	27.7 [24.8–30.8]	56	26.6 [25.8–29.8]	0.499
Diabetes mellitus, n (%)	269	61 (22.7%)	62	9 (14.5%)	0.156
Prediabetes ^a , n (%)	269	51 (19.0%)	62	12 (19.4%)	0.943
Family history of CAD, n (%)	269	119 (44.2%)	62	33 (53.2%)	0.200
Typical angina pectoris, n (%)	269	91 (33.8%)	62	19 (30.7%)	0.631
NYHA class	166		30		0.762
I		77 (46.4%)		18 (19.0%)	
II		79 (47.6%)		11 (36.7%)	
III		10 (6.0%)		1 (3.3%)	
Agatston Coronary Calcium Score	227	656 [293–1419]	80	194 [40–576]	<0.001
Referral for ICA (within 6 months), n (%)	269	184 (68.4%)	62	22 (35.5%)	<0.001
Early revascularization (within 6 months, PCI or CABG), n (%)	269	137 (50.9%)	62	11 (17.7%)	<0.001
Early PCI (within 6 months), n (%)	269	108 (40.2%)	62	10 (16.1%)	<0.001
Early CABG (within 6 months), n (%)	269	32 (11.9%)	62	1 (1.6%)	0.015
Medication					
Antiplatelet drug (Aspirin or other), n (%)	269	166 (61.7%)	62	26 (41.9%)	0.004
Anticoagulation, n (%)	269	20 (7.4%)	62	5 (8.1%)	0.866
Lipid-lowering drug, n (%)	269	160 (59.5%)	62	29 (46.8%)	0.068
Betablocker, n (%)	269	155 (57.6%)	62	29 (46.8%)	0.121
Long-acting nitrate, n (%)	269	33 (12.3%)	62	11 (17.7%)	0.252
Calcium channel blocker, n (%)	269	55 (20.5%)	62	10 (16.1%)	0.440
ACE inhibitor, n (%)	269	62 (23.1%)	62	12 (19.4%)	0.529
AT II antagonist, n (%)	269	68 (25.3%)	62	18 (29.0%)	0.543
Diuretic, n (%)	269	61 (22.7%)	62	14 (22.6%)	0.987
Antiarrhythmic drug, n (%)	269	7 (2.6%)	62	2 (3.2%)	0.785
AI-QCT					
AI-QCT diameter stenosis, %	269	72 [60–79]	62	36 [27–43]	<0.001
AI-QCT diameter stenosis \geq 30%, n (%)	269	269 (100%)	62	44 (71.0%)	<0.001
AI-QCT diameter stenosis \geq 50%, n (%)	269	256 (95.2%)	62	9 (14.5%)	<0.001
AI-QCT diameter stenosis \geq 70%, n (%)	269	163 (60.6%)	62	0 (0.0%)	<0.001
Vessels with AI-QCT diameter stenosis \geq 50% ^b , n (%)					
LM	262	13 (5.0%)	61	0 (0.0%)	0.076
LAD	269	215 (79.9%)	62	5 (8.1%)	<0.001
LCX	269	93 (34.6%)	62	1 (1.6%)	<0.001
RCA	269	139 (51.7%)	62	4 (6.5%)	<0.001
Area stenosis, %	269	92 [85–96]	62	58 [47–69]	<0.001
Percent atheroma volume, %	269	18.9 [11.5–27.1]	62	7.9 [4.1–13.2]	<0.001
Percent calcified plaque volume, %	269	6.8 [3.1–12.6]	62	2.0 [0.9–6.1]	<0.001
Percent non-calcified plaque volume, %	269	10.1 [7.5–14.6]	62	5.6 [3.0–8.1]	<0.001
Positive remodeling ^c , n (%)	269	269 (100%)	62	62 (100%)	-
Total vessel volume, mm ³	269	3209 [2677–3838]	62	3167 [2797–3167]	0.840
Total lumen volume, mm ³	269	2520 [2073–3017]	62	2856 [2439–3310]	<0.001
Total vessel length, mm	269	638 \pm 104	62	638 \pm 83	0.800

Values are n (%), mean \pm standard deviation (SD), or median [interquartile range (IQR)]. P-values are from Mann Withney U tests, T-tests, or Chi-square tests.

^a Prediabetes was defined as HbA1c 6.0–6.5%, or fasting glucose 6.1–6.9 mmol/l or impaired glucose tolerance (2 h plasma glucose 7.8–11.0 mmol/l in a 75 oral glucose tolerance test).

^b Including side branches with diameter \geq 1.5 mm. In some patients, left main was either absent or too short to be assessed as separate segment.

^c Remodeling index \geq 1.1. Percent plaque volume (%) = plaque volume (mm³)/vessel volume (mm³)*100. AI-QCT = artificial intelligence quantitative computed tomography, ACE = angiotensin converting enzyme, AP = angina pectoris, AT II = angiotensin II, BMI = body mass index, CABG = coronary artery bypass grafting, CAD = coronary artery disease, ICA = invasive coronary angiography, LAD = left anterior descending, LCX = left circumflex artery, LM = left main artery, NYHA = New York Heart Association, PCI = percutaneous coronary intervention, PET = positron emission tomography, RCA = right coronary artery.

4. Discussion

This was a retrospective, single-center, observational cohort study to assess the prognostic value for long-term clinical events of a novel AI-based coronary CTA-derived ischemia algorithm (AI-QCT_{ischemia}) among patients with visually obstructive CAD on coronary CTA referred to downstream PET perfusion imaging for hemodynamic assessment of CAD. The main findings of this study are, that among patients with normal PET perfusion, an abnormal AI-QCT_{ischemia} result was associated with a 2.5-fold higher adjusted rate of all-cause death, MI, or uAP throughout 6.2 median years of follow-up. In contrast, incremental risk stratification was not observed for patients with myocardial ischemia on PET perfusion imaging.

4.1. Combined anatomical and functional imaging of CAD with coronary CTA

AI-QCT_{ischemia} as a novel AI-based algorithm aims at overcoming the limitations of coronary CTA as an anatomical test only, by estimating the presence of ischemia directly from the coronary CTA images.¹¹ With the potential adoption of this algorithm into the clinical workflow, anatomical, morphological, and functional information could be gained from one single coronary CTA scan. In this study, we investigated the added prognostic value of AI-QCT_{ischemia} according to the PET perfusion result among patients with visually obstructive CAD.

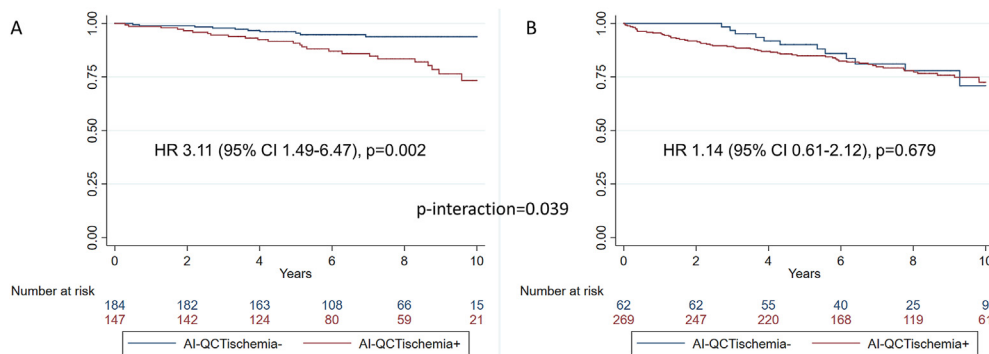


Fig. 3. Kaplan-Meier Curves of the Primary Endpoint in Patients with Normal or Abnormal PET Perfusion. Crude Kaplan-Meier Curves of the primary endpoint death, myocardial infarction (MI), and unstable angina pectoris (uAP) among patients with A) normal positron emission tomography (PET) perfusion, and B) abnormal PET perfusion. AI-QCT^{ischemia}-denotes normal and AI-QCT^{ischemia}+ denotes abnormal AI-QCT^{ischemia} result. AI-QCT = artificial intelligence quantitative computed tomography, CI = confidence interval, HR = hazard ratio.

Table 3

Cox regressions for the primary endpoint and components at 10 Years.

Patients with	Crude hazard ratios				Adjusted hazard ratios			
	Abnormal AI-QCT ^{ischemia} result (N = 147)	Normal AI-QCT ^{ischemia} result (N = 184)	HR (95% CI)	p-value	N Patients	N Events	HR (95% CI) adjusted	p-value adjusted
Patients with normal PET perfusion (N = 331)								
Death, MI, uAP, n (%)	25 (17.0%)	10 (5.4%)	3.11 (1.49–6.47)	0.002	331	35	2.47 (1.17–5.21) ¹	0.018 ¹
Death, n (%)	14 (9.5%)	7 (3.8%)	2.37 (0.95–5.88)	0.064	331	21	2.27 (0.91–5.64) ²	0.077 ²
MI, n (%)	12 (8.2%)	3 (1.7%)	5.08 (1.43–18.00)	0.012	331	15	3.93 (1.10–14.07) ³	0.036 ³
uAP, n (%)	3 (2.0%)	0 (0.0%)	–	–	331	3	–	–
Patients with abnormal PET perfusion (N = 331)								
Death, MI, uAP, n (%)	59 (21.9%)	12 (19.4%)	1.14 (0.61–2.12)	0.679	331	71	1.09 (0.58–2.02) ³	0.794 ³
Death, n (%)	30 (11.2%)	11 (17.7%)	0.57 (0.28–1.13)	0.108	331	41	0.55 (0.27–1.10) ⁴	0.091 ⁴
MI, n (%)	21 (8.2%)	1 (1.6%)	4.83 (0.65–35.93)	0.124	331	22	–	–
uAP, n (%)	17 (6.3%)	0 (0.05)	–	–	331	17	–	–

Displayed are numbers (percentage) of first events and hazard ratios (HR) with 95% confidence intervals (CI) from Cox proportional hazards models. Results were adjusted for variables with a significant association with the reported endpoints in univariable Cox regressions (Tables S2–4): 1) age, diabetes mellitus; 2) diabetes mellitus (only strongest univariable predictor due to the limited event number); 3) age, 4) age, smoking. AI-QCT = artificial intelligence quantitative computed tomography, MI = myocardial infarction, PET = positron emission tomography, uAP = unstable angina pectoris.

There are currently two other CT-based approaches to detect functionally significant stenosis, i.e. FFR-CT and myocardial CT perfusion imaging. FFR-CT is a computational fluid-dynamic based approach to model invasive FFR from coronary CTA.²² FFR-CT has demonstrated robust prognostic value,^{23,24} significant impact on clinical decision making,²⁵ and is already used in clinical practice in some sites.^{26,27} However, the availability of larger scale real world data²⁶ has recently raised concerns about its diagnostic performance outside study settings, that is substantially lower as in the validation studies.^{28,29} Also, intention-to-diagnose analyses have shown, that FFR-CT was interpretable in 83% of major coronary arteries, resulting in only 75% of patients with an evaluable 3-vessel result.³⁰ This issue is not evident from analyses, where poor CTA quality has been an upfront exclusion criterion and the reported scan rejection rate was only 3%.²⁵ Myocardial CT perfusion imaging³¹ requires a specific imaging protocol, is associated with increased radiation, and there is currently no consensus on the threshold to determine abnormal MBF. So far, these factors have hindered the integration of myocardial CT perfusion imaging into routine clinical practice.

AI-QCT^{ischemia} is an approach to determine ischemia from coronary CTA fully based on AI without the need for computational fluid dynamics. Having recently received clearance by the FDA, and in the light of the globally growing number of patients undergoing coronary CTA,³² as well as growing applications of coronary CTA across various clinical scenarios,³³ AI-QCT^{ischemia}, if reliable, may carry the potential to affect the diagnostic pathway of CAD at large. Therefore, we performed a study

to investigate its prognostic potential in a typical population that needs downstream ischemia testing after coronary CTA.

4.2. Prognostic value of AI-QCT^{ischemia}

Selective hybrid coronary CTA/¹⁵O-H₂O-PET imaging¹² and pooled quantitative PET perfusion across various radiotracers³⁴ have proven prognostic value. Also, plaque burden according to AI-QCT has been shown to be independently associated with 10-year cardiovascular outcomes.⁷ In the external validation cohort of AI-QCT^{ischemia}, among 208 patients from the PACIFIC trial, AI-QCT^{ischemia} was an independent predictor of major adverse cardiovascular events on top of clinical factors and obstructive disease throughout 8.5 years of follow-up.¹¹ In a previous report from this cohort, AI-QCT^{ischemia} proved to be an independent predictor for death, MI, or uAP. This risk stratification pertained specifically to patients with no or non-obstructive anatomical disease (visual stenosis ≤50%).¹⁴

In the current study we have extended these previous findings by investigating the prognostic value of AI-QCT^{ischemia} among patients with visually obstructive disease and normal or abnormal ¹⁵O-H₂O-PET perfusion. We found that, among patients with normal PET perfusion, an abnormal AI-QCT^{ischemia} result identified those patients with a higher event risk, despite on average 2 years younger patients, as well as equally prevalent cardiovascular risk factors and medical therapy in both AI-QCT^{ischemia} groups. The prognostic power of AI-QCT^{ischemia} accrued over the long-term with event rates diverging from 6 years of follow-up

onwards.

Of note, only 63% of the total study population had $\geq 50\%$ diameter stenosis according to AI-QCT. This is in line with a previous report, that stenosis assessment with AI-QCT vs. visual analysis generally leads to a downgrade in stenosis severity.³⁵ However, the findings of the current study support the concept, that the prognostic value of AI-QCT_{ischemia} is not only related to the more accurate diagnosis of obstructive CAD by AI-QCT vs. visual analysis, because in both PET perfusion groups, where AI-QCT_{ischemia} had different prognostic value, $\sim 94\text{--}95\%$ of patients with abnormal AI-QCT_{ischemia} result had AI-QCT diameter stenosis $\geq 50\%$. But, since AI-QCT diameter stenosis is the highest ranked feature in the AI-QCT_{ischemia} algorithm,¹¹ the prognostic value of AI-QCT diameter stenosis vs. AI-QCT_{ischemia} should be the target of future studies in unselected populations.

95% of patients with normal PET perfusion, where AI-QCT_{ischemia} showed incremental risk stratification, did not undergo early revascularization. In contrast, in the abnormal PET perfusion group, where no additional risk stratification by AI-QCT_{ischemia} was found, 45% underwent early revascularization, and antiplatelet therapy was more frequently prescribed in patients with an abnormal AI-QCT_{ischemia} result. In the total study population, outcomes for non-revascularized vs. revascularized patients were generally similar, in agreement with prior analysis from this registry.¹² To account for revascularization, we performed a sensitivity analysis among patients without early revascularization. The main results of the study remained unchanged when excluding patients that underwent early revascularization. The risk stratification by AI-QCT_{ischemia} in the normal PET perfusion group was numerically even slightly increased after excluding patients that underwent revascularization. This is also in line with our previous report, that AI-QCT_{ischemia} showed pronounced prognostic value among patients not undergoing early revascularization.¹⁴ However, only a dedicated randomized-controlled trial would be able to clarify, whether revascularization improves outcomes in patients with an abnormal AI-QCT_{ischemia} result. Alternatively, since AI-QCT_{ischemia} is derived from the epicardial atherosclerotic burden on coronary CTA, rather more aggressive medical therapy could be warranted given the higher burden of non-obstructive or non-flow-limiting atherosclerotic disease, known to be related to poor clinical outcome.^{36,37}

4.3. AI-QCT_{ischemia} vs. ¹⁵O-H₂O PET perfusion

In the total cohort, 50% of the patients had “ischemia” according to PET and 63% according to AI-QCT_{ischemia}, but these two techniques disagreed in 32% of the patients. It has been acknowledged previously, that some CTA-derived plaque parameters like non-calcified plaque volume or positive remodeling are independently associated with impaired MBF on PET and invasive FFR, while others, like low-attenuation plaque or spotty calcification, are only associated with impaired invasive FFR, but not with PET.³⁸ Thus, varying phenotypes of atherosclerosis may impact myocardial perfusion imaging and FFR in different ways. Since AI-QCT_{ischemia} uses AI to detect atherosclerosis features from coronary CTA that have a certain probability to be found in a lesion with invasive FFR ≤ 0.80 , some disagreement between AI-QCT_{ischemia} and PET is consistent with the current evidence. Furthermore, in contrast to AI-QCT_{ischemia} which was trained to detect flow-limiting atherosclerosis from coronary CTA, PET detects myocardial perfusion abnormalities that are not only caused by epicardial but also microvascular disease. And since both, microvascular³⁹ and epicardial CAD^{36,37} are known to be associated with impaired prognosis, it could be hypothesized, that these techniques may act complementary. This is also supported by the current data showing that the event rate for patients with preserved PET perfusion but an abnormal AI-QCT_{ischemia} result was close to those with abnormal PET perfusion. These patients indeed proved to have more advanced epicardial atherosclerosis, as evidenced by higher plaque burden (PAV, CPV, and NCPV), more severe lumen impairment (diameter stenosis, area stenosis, lumen volume), and more

frequent positive remodeling. However, while AI-QCT_{ischemia} successfully risk stratifies patients with normal PET perfusion, among the patients with abnormal PET perfusion, $\sim 20\%$ experienced the primary endpoint regardless of the AI-QCT_{ischemia} result. Therefore, the detailed underlying factors to the discrepancies between PET perfusion and AI-QCT_{ischemia} require future dedicated investigation. Also, appropriate prospective studies are warranted to test the impact of AI-QCT_{ischemia} on outcomes in unselected populations.

4.4. Limitations

The results of this study must be considered in the light of several limitations. It was a single-center, observational study associated with all limitations of a retrospective analysis. However, for AI-QCT_{ischemia}, the CTAs were re-analyzed blinded to clinical data, PET perfusion results, and outcome. The study population represents a highly selected cohort of symptomatic patients having visually obstructive CAD on a coronary CTA referred for downstream ischemia testing with PET perfusion imaging, and the results do not pertain to patients without obstructive CAD on coronary CTA or those undergoing PET perfusion imaging for another indication. The clinical coronary CTA reading as basis for PET perfusion referral was performed visually by experienced clinical readers. Therefore, intra- or interobserver reproducibility in stenosis assessment, that could have introduced variability in the current analysis, was not assessed. The clinical CTA reading was performed according to the AHA recommendations valid during the enrolment period.¹⁶ However, the segmenting system used should not impact the overall interpretation of the coronary CTA scan. AI-QCT_{ischemia} is binary and does currently not quantify the magnitude of ischemia. Invasive FFR was not routinely performed, as the patients had non-invasive functional information available based on PET.

5. Conclusions

Among patients with visually obstructive CAD on coronary CTA and normal downstream PET perfusion, an abnormal AI-QCT_{ischemia} result was associated with a 2.5-fold increased adjusted rate of long-term death, MI, or uAP. This incremental risk stratification did not pertain to patients with abnormal PET perfusion.

Funding

The study was funded by the Finnish Foundation for Cardiovascular Research and Finnish State Research Funding [VTR 13403]. Dr. Bär was supported by the Swiss National Science Foundation [P500PM_210788] and the University of Turku, Finland. Cleerly Inc. performed the image analysis without costs.

Data availability statement

The data underlying this article may be shared upon reasonable request from the corresponding author.

Declaration of competing interest

Dr. Bär received research grants to the institution from Medis Medical Imaging Systems, Bangerter-Rhyner Stiftung (Basel, Switzerland) and Abbott, outside the submitted work. Dr. Saraste received consultancy fees from Astra Zeneca and Pfizer, and speaker fees from Abbott, Astra Zeneca, Janssen, Novartis and Pfizer. Dr. Bax received speaker fees from Abbott. Drs Earls and Min are employees of and hold equity in Cleerly Inc. Dr. Knuuti received consultancy fees from GE Healthcare and Syntekit and speaker fees from Bayer, Lundbeck, Boehringer-Ingelheim, Pfizer and Siemens, outside of the submitted work. All other authors have reported that they have no relationships relevant to the contents of this paper to disclose.

Appendix A. Supplementary data

Supplementary data to this article can be found online at <https://doi.org/10.1016/j.jcct.2024.04.001>.

References

- Knuuti J, Wijns W, Saraste A, et al. 2019 ESC Guidelines for the diagnosis and management of chronic coronary syndromes. *Eur Heart J*. 2020;41:407–477. <https://doi.org/10.1093/eurheartj/ehz425>.
- Gulati M, Levy PD, Mukherjee D, et al. AHA/ACC/AASE/CHEST/SAEM/SCCT/SCMR guideline for the evaluation and diagnosis of chest Pain: a report of the American college of cardiology/American heart association joint committee on clinical practice guidelines. *Circulation*. 2021;16:54–122. <https://doi.org/10.1161/CIR.0000000000001029>, 2021.
- Choi AD, Marques H, Kumar V, et al. CT evaluation by artificial intelligence for atherosclerosis, stenosis and vascular morphology (CLARIFY): a multi-center, international study. *J Cardiovasc Comput Tomogr*. 2021;15:470–476. <https://doi.org/10.1016/j.jcct.2021.05.004>.
- Griffin WF, Choi AD, Riess JS, et al. AI evaluation of stenosis on coronary CTA, Comparison with quantitative coronary angiography and fractional flow reserve. *JACC Cardiovasc Imaging*. 2023;16:193–205. <https://doi.org/10.1016/j.jcmg.2021.10.020>.
- Lipkin I, Telluri A, Kim Y, et al. Coronary CTA with AI-QCT interpretation: Comparison with myocardial perfusion imaging for detection of obstructive stenosis using invasive angiography as reference standard. *AJR Am J Roentgenol*. 2022;219:407–419. <https://doi.org/10.2214/AJR.21.27289>.
- Jonas R, Earls JP, Marques H, et al. Relationship of age, atherosclerosis and angiographic stenosis using artificial intelligence. *Open Heart*. 2021;8:e001832. <https://doi.org/10.1136/openhrt-2021-001832>.
- Nurmohamed NS, Bom MJ, Jukema RA, et al. AI-guided quantitative plaque staging predicts long-term cardiovascular outcomes in patients at risk for atherosclerotic CVD. *JACC Cardiovascular Imaging*. 2024;17:269–280. <https://doi.org/10.1016/j.jcmg.2023.05.020>.
- United States Food and Drug Administration. Cleerly ISCHEMIA. Cleerly ISCHEMIA. https://www.accessdata.fda.gov/cdrh_docs/pdf23/K231335.pdf. Accessed December 11, 2023.
- Stuijzand WJ, van Rosendaal AR, Lin FY, et al. Stress myocardial perfusion imaging vs coronary computed tomographic angiography for diagnosis of invasive vessel-specific coronary physiology: predictive modeling results from the computed tomographic evaluation of atherosclerotic determinants of myocardial ischemia (CRENCE) trial. *JAMA Cardiol*. 2020;5:1338–1348. <https://doi.org/10.1001/jamacardio.2020.3409>.
- Danad I, Rajmakers PG, Driessen RS, et al. Comparison of coronary CT angiography, SPECT, PET, and hybrid imaging for diagnosis of ischemic heart disease determined by fractional flow reserve. *JAMA Cardiol*. 2017;2:1100. <https://doi.org/10.1001/jamacardio.2017.2471>.
- Nurmohamed NS, Danad I, Jukema RA, et al. Development and validation of a quantitative coronary CT angiography model for diagnosis of vessel-specific coronary ischemia. March 13 *JACC Cardiovascular Imaging*. 2024. <https://doi.org/10.1016/j.jcmg.2024.01.007> [ePub ahead of print].
- Maaniitty T, Stenström I, Bax JJ, et al. Prognostic value of coronary CT angiography with selective PET perfusion imaging in coronary artery disease. *JACC Cardiovascular Imaging*. 2017;10:1361–1370. <https://doi.org/10.1016/j.jcmg.2016.10.025>.
- Stenström I, Maaniitty T, Uusitalo V, et al. Absolute stress myocardial blood flow after coronary CT angiography guides referral to invasive angiography. *JACC Cardiovascular Imaging*. 2019;12(11, Part 1):2266–2267. <https://doi.org/10.1016/j.jcmg.2019.08.002>.
- Bär S, Nabeta T, Maaniitty T, et al. Prognostic value of a novel artificial intelligence-based coronary computed tomography angiography-derived ischaemia algorithm for patients with suspected coronary artery disease. *Eur Heart J Cardiovasc Imaging*. December 12, 2023;jead339. <https://doi.org/10.1093/ehjci/jead339> [ePub ahead of print].
- Kajander S, Joutsiniemi E, Saraste M, et al. Cardiac positron emission tomography/computed tomography imaging accurately detects anatomically and functionally significant coronary artery disease. *Circulation*. 2010;122:603–613. <https://doi.org/10.1161/CIRCULATIONAHA.109.915009>.
- Austen W, Edwards J, Frye R, et al. A reporting system on patients evaluated for coronary artery disease. Report of the ad hoc committee for grading of coronary artery disease, council on cardiovascular surgery, American heart association. *Circulation*. 1975;51:5–40. <https://doi.org/10.1161/01.CIR.51.4.5>.
- Cerqueira MD, Weissman NJ, Dilsizian V, et al. American heart association writing group on myocardial segmentation and registration for cardiac imaging. Standardized myocardial segmentation and nomenclature for tomographic imaging of the heart. A statement for healthcare professionals from the cardiac imaging committee of the council on clinical cardiology of the American heart association. *Int J Cardiovasc Imag*. 2002;18:539–542.
- Danad I, Uusitalo V, Kero T, et al. Quantitative assessment of myocardial perfusion in the detection of significant coronary artery disease: cutoff values and diagnostic accuracy of quantitative [15O]H₂O PET imaging. *J Am Coll Cardiol*. 2014;64:1464–1475. <https://doi.org/10.1016/j.jacc.2014.05.069>.
- Leipsic J, Abbara S, Achenbach S, et al. SCCT guidelines for the interpretation and reporting of coronary CT angiography: a report of the Society of Cardiovascular Computed Tomography Guidelines Committee. *J Cardiovasc Comput Tomogr*. 2014;8:342–358. <https://doi.org/10.1016/j.jcct.2014.07.003>.
- Thygesen K, Alpert JS, Jaffe AS, et al. Fourth universal definition of myocardial infarction (2018). *Eur Heart J*. 2019;40:237–269. <https://doi.org/10.1093/eurheartj/ehy462>.
- Byrne RA, Rossello X, Coughlan JJ, et al. ESC Scientific Document Group. 2023 ESC Guidelines for the management of acute coronary syndromes: developed by the task force on the management of acute coronary syndromes of the European Society of Cardiology (ESC). *Eur Heart J*. 2023;44:3720–3826. <https://doi.org/10.1093/eurheartj/ehad191>.
- Taylor CA, Fonte TA, Min JK. Computational fluid dynamics applied to cardiac computed tomography for noninvasive quantification of fractional flow reserve. *J Am Coll Cardiol*. 2013;61:2233–2241. <https://doi.org/10.1016/j.jacc.2012.11.083>.
- Nørgaard BL, Gaur S, Fairbairn TA, et al. Prognostic value of coronary computed tomography angiographic derived fractional flow reserve: a systematic review and meta-analysis. *Heart*. 2022;108:194–202. <https://doi.org/10.1136/heartjnl-2021-319773>.
- Ishayhid AR, Nørgaard BL, Gaur S, et al. Prognostic value and risk continuum of noninvasive fractional flow reserve derived from coronary CT angiography. *Radiology*. 2019;292:343–351. <https://doi.org/10.1148/radiol.2019182264>.
- Fairbairn TA, Nieman K, Akasaka T, et al. Real-world clinical utility and impact on clinical decision-making of coronary computed tomography angiography-derived fractional flow reserve: lessons from the ADVANCE Registry. *Eur Heart J*. 2018;39:3701–3711. <https://doi.org/10.1093/eurheartj/ehy530>.
- Mittal TK, Hothi SS, Venugopal V, et al. The use and efficacy of FFR-CT: real-world multicenter audit of clinical data with cost analysis. *JACC Cardiovascular Imaging*. 2023;16:1056–1065. <https://doi.org/10.1016/j.jcmg.2023.02.005>.
- Graby J, Metters R, Kandan SR, et al. Real-world clinical and cost analysis of CT coronary angiography and CT coronary angiography-derived fractional flow reserve (FFRCT)-guided care in the National Health Service. *Clin Radiol*. 2021;76:862.e19–862.e28. <https://doi.org/10.1016/j.crad.2021.06.009>.
- Min JK, Taylor CA, Achenbach S, et al. Noninvasive fractional flow reserve derived from coronary CT angiography: clinical data and scientific principles. *JACC Cardiovascular Imaging*. 2015;8:1209–1222. <https://doi.org/10.1016/j.jcmg.2015.08.006>.
- Nørgaard BL, Leipsic J, Gaur S, et al. NXT Trial Study Group. Diagnostic performance of noninvasive fractional flow reserve derived from coronary computed tomography angiography in suspected coronary artery disease: the NXT trial (Analysis of Coronary Blood Flow Using CT Angiography: next Steps). *J Am Coll Cardiol*. 2014;63:1145–1155. <https://doi.org/10.1016/j.jacc.2013.11.043>.
- Driessen RS, Danad I, Stuijzand WJ, et al. Comparison of coronary computed tomography angiography, fractional flow reserve, and perfusion imaging for ischemia diagnosis. *J Am Coll Cardiol*. 2019;73:161–173. <https://doi.org/10.1016/j.jacc.2018.10.056>.
- Danad I, Szymoniak J, Schulman-Marcus J, Min JK. Static and dynamic assessment of myocardial perfusion by computed tomography. *Eur Heart J Cardiovasc Imaging*. 2016;17:836–844. <https://doi.org/10.1093/ehjci/jew044>.
- Reeves RA, Halpern EJ, Rao VM. Cardiac imaging trends from 2010 to 2019 in the medicare population. *Radiol Cardiothorac Imaging*. 2021;3:e210156. <https://doi.org/10.1148/ryct.2021210156>.
- Serruys PW, Kotoku N, Nørgaard BL, et al. Computed tomographic angiography in coronary artery disease. *EuroIntervention*. 2023;18:e1307–e1327. <https://doi.org/10.4244/EIJ-D-22-00776>.
- Juárez-Orozco LE, Tio RA, Alexanderson E, et al. Quantitative myocardial perfusion evaluation with positron emission tomography and the risk of cardiovascular events in patients with coronary artery disease: a systematic review of prognostic studies. *Eur Heart J Cardiovasc Imaging*. 2018;19:1179–1187. <https://doi.org/10.1093/ehjci/jex331>.
- Nurmohamed NS, Cole JH, Budoff MJ, et al. Impact of atherosclerosis imaging-quantitative computed tomography on diagnostic certainty, downstream testing, coronary revascularization, and medical therapy: the CERTAIN study. *Eur Heart J Cardiovasc Imaging*. January 25, 2024;jeae029. <https://doi.org/10.1093/ehjci/jeae029> [ePub ahead of print].
- Min JK, Dunning A, Lin FY, et al. Age- and sex-related differences in all-cause mortality risk based on coronary computed tomography angiography findings results from the International Multicenter CONFIRM (Coronary CT Angiography Evaluation for Clinical Outcomes: an International Multicenter Registry) of 23,854 patients without known coronary artery disease. *J Am Coll Cardiol*. 2011;58:849–860. <https://doi.org/10.1016/j.jacc.2011.02.074>.
- Nielsen LH, Bøtker HE, Sørensen HT, et al. Prognostic assessment of stable coronary artery disease as determined by coronary computed tomography angiography: a Danish multicentre cohort study. *Eur Heart J*. 2017;38:413–421. <https://doi.org/10.1093/eurheartj/ehw548>.
- Driessen RS, Stuijzand WJ, Rajmakers PG, et al. Effect of plaque burden and morphology on myocardial blood flow and fractional flow reserve. *J Am Coll Cardiol*. 2018;71:499–509. <https://doi.org/10.1016/j.jacc.2017.11.054>.
- Del Buono MG, Montone RA, Camilli M, et al. Coronary microvascular dysfunction across the spectrum of cardiovascular diseases. *J Am Coll Cardiol*. 2021;78:1352–1371. <https://doi.org/10.1016/j.jacc.2021.07.042>.